

QCD corrections to J/ψ plus Z^0 -boson production at the LHC

Song Mao^a, Ma Wen-Gan^a, Li Gang^b, Zhang Ren-You^a, and Guo Lei^a

^a*Department of Modern Physics, University of Science and Technology of China, Hefei, Anhui 230026, P.R.China*

^b*School of Physics and Material Science, Anhui University, Hefei, Anhui 230039, P.R.China*

E-mail: songmao@mail.ustc.edu.cn , mawg@ustc.edu.cn,

lig2008@mail.ustc.edu.cn, zhangry@ustc.edu.cn, guolei@mail.ustc.edu.cn

ABSTRACT: The $J/\psi + Z^0$ associated production at the LHC is an important process in investigating the color-octet mechanism of non-relativistic QCD in describing the processes involving heavy quarkonium. We calculate the next-to-leading order (NLO) QCD corrections to the $J/\psi + Z^0$ associated production at the LHC within the factorization formalism of nonrelativistic QCD, and provide the theoretical predictions for the distribution of the J/ψ transverse momentum. Our results show that the differential cross section at the leading-order is significantly enhanced by the NLO QCD corrections. We conclude that the LHC has the potential to verify the color-octet mechanism by measuring the $J/\psi + Z^0$ production events.

KEYWORDS: Hadronic Colliders, NLO Computations, Heavy Quark Physics

PACS: 12.38.Bx, 12.39.St, 14.70.Hp, 13.85.-t .

Contents

1. Introduction	1
2. LO calculations for the $pp \rightarrow J/\psi + Z^0 + X$ process	3
3. NLO QCD corrections to the $pp \rightarrow J/\psi + Z^0 + X$ process	4
3.1 virtual corrections	4
3.2 Real gluon/light-(anti)quark emission corrections	5
3.3 NLO QCD corrected cross sections	7
4. Numerical results and discussion	8
5. Summary	10

1. Introduction

Since the discovery of the first charm-anticharm bound state J/ψ , the study of quarkonium is a very interesting topic in both a theoretical and an experimental point of view, which provide a good place to probe both perturbative and non-perturbative aspects of QCD dynamics.

In the early days of quarkonium physics, the production and decay of a quarkonium was described by the color-singlet mechanism (CSM) [1–5] with the color-singlet $Q\bar{Q}$ pair having the appropriate spin, angular-momentum and charge conjugation quantum numbers, and it was assumed that the decay and production of a quarkonium can be factorized into a short distance part, which can be calculated in a perturbative series of the running coupling constant $\alpha_s(M)$, and a long distance part, which relies on the nonperturbative dynamics of the bound state. However, the CSM has encounter many difficulties in various theoretical [6–11] and experimental aspects [12,13], such as the appearance of a logarithmic infrared divergence in the case of NLO P -wave decays into light hadrons and the huge discrepancy of the high- p_t J/ψ production between the theoretical prediction and the experimental measurement at the Tevatron.

In 1995, the nonrelativistic QCD (NRQCD) [14], proposed by Bodwin, Braaten and Lepage (BBL), provides a rigorous theoretical framework for the description of heavy-quarkonium production and decay. In the NRQCD, the idea of perturbative factorization is retained, the process of production and decay of heavy quarkonium is separated into two parts: short distance part, which allows the intermediate $Q\bar{Q}$ pair with quantum numbers different from those of the physical quarkonium state, and the long distance matrix elements (LDMEs), which can be extracted from experiments. The relative importance of

the LDMEs can be estimated by means of the velocity scaling rules [15]. If one only retains the lowest order in v , the description of S -wave quarkonia production or annihilation reduces to the CSM. In the case of P -waves, infrared singularities which appear in some of the short distance coefficients can be absorbed into the long distance part of color-octet S -wave states. Including the contribution of color-octet states, the large discrepancies between the experimental data of J/ψ production at the Tevatron and the theoretical predictions based on CSM successfully reconciled [16–19].

Recently, substantial progress has been achieved in the calculation of high order QCD corrections to J/ψ hadroproduction in order to clarify the validity and limitation of the NRQCD formalism. The DELPHI data more favor the NRQCD color-octet mechanism (COM) predictions for the $\gamma\gamma \rightarrow J/\psi + X$ process [20,21]. Similarly the recent experimental data on the J/ψ photoproduction of H1 [22] are fairly well described by the complete NLO NRQCD corrections [23], and give strong support to the existence of the COM. However, At B-factories, a series of processes was calculated up to the QCD NLO corrections in the CSM [24–34]. Together with the relativistic correction [35–39], it seems that most experimental data could be understood. Additionally, the J/ψ polarization in hadroproduction at the Tevatron [40,41] and photoproduction at the HERA [42] also conflict with the NRQCD predictions. Therefore, the J/ψ production mechanism is still a big challenge. The further tests for the CSM and COM in NRQCD are still needed on the production of heavy quarkonium.

In order to investigate the effects of the COM in heavy quarkonium production, it is an urgent task to study the processes which heavily depend on the production mechanism. The J/ψ production associated with a gauge boson at the LHC, is a suitable process for studying COM. In high energy collider experiments, W^\pm , Z^0 and J/ψ can be identified by using their purely leptonic decays [43,44], which are particularly useful in hadron colliders, because they provide an enormous suppression of the background. In reference [45], the authors give a theoretical prediction at the LO for associated production of heavy quarkonium and electroweak bosons at hadron colliders. The numerical results show that for $J/\psi + \gamma$ associated production the CSM provides the main contribution, but for $J/\psi + W$ and $J/\psi + Z^0$ associated production, the COM contribution to the cross section is dominative. The NLO QCD corrections to $pp \rightarrow J/\psi + \gamma$ production in the CSM were provided in [46], and the results show that the cross section in large p_T region of J/ψ can be enhanced by two orders in magnitude. Recently, the complete NLO QCD corrections to $J/\psi + W$ were calculated at the LHC in nonrelativistic quantum chromodynamics [47]. There only the color-octet contributes to the process $pp \rightarrow J/\psi + W$ at both LO and QCD NLO. The numerical results show that the differential cross section at the LO is significantly enhanced by the NLO QCD corrections. In this paper we calculate the NLO QCD corrections to the associated J/ψ production with a Z^0 gauge boson in the NRQCD at the LHC, and present the theoretical predictions for the p_T distribution of J/ψ .

This paper is structured as follows: In Sec. II we give the calculation description of the LO cross section for the $pp \rightarrow J/\psi + Z^0 + X$ process, and the calculations of the NLO QCD corrections are provided in Sec. III. In Sec. IV we present some numerical results and discussion, and finally a short summary is given.

2. LO calculations for the $pp \rightarrow J/\psi + Z^0 + X$ process

At the LO, there involves two types of partonic processes, which contribute to the $pp \rightarrow J/\psi + Z^0 + X$ process:

$$q\bar{q} \rightarrow c\bar{c}[n] + Z^0, n = {}^1S_0^{(8)}, {}^3S_1^{(8)}, {}^3P_J^{(8)}, \quad (2.1)$$

$$gg \rightarrow c\bar{c}[n] + Z^0, n = {}^3S_1^{(1)}, {}^1S_0^{(8)}, {}^3S_1^{(8)}, {}^3P_J^{(8)}, \quad (2.2)$$

where q represents all possible light-quarks (u, d and s). The tree-level Feynman diagrams are shown in Fig.1. The cross section for the production of a $c\bar{c}$ pair in a Fock state n , $\hat{\sigma}[ij \rightarrow c\bar{c}[n] + Z^0]$, is calculated from the amplitudes which are obtained by applying certain projectors onto the usual QCD amplitudes for open $c\bar{c}$ production. In the notations of Ref. [48]:

$$\mathcal{A}_{c\bar{c}[{}^1S_0^{(8)}]} = \text{Tr} \left[\mathcal{C}_8 \Pi_0 \mathcal{A} \right]_{q=0},$$

$$\mathcal{A}_{c\bar{c}[{}^3S_1^{(1/8)}]} = \mathcal{E}_\alpha \text{Tr} \left[\mathcal{C}_{1/8} \Pi_1^\alpha \mathcal{A} \right]_{q=0},$$

$$\mathcal{A}_{c\bar{c}[{}^3P_J^{(8)}]} = \mathcal{E}_{\alpha\beta}^{(J)} \frac{d}{dq_\beta} \text{Tr} \left[\mathcal{C}_8 \Pi_1^\alpha \mathcal{A} \right]_{q=0},$$

where \mathcal{A} denotes the QCD amplitude with amputated charm spinors, the lower index q represents the momentum of the heavy quark in the $Q\bar{Q}$ rest frame. $\Pi_{0/1}$ are spin projectors onto the spin singlet and spin triplet states. $\mathcal{C}_{1/8}$ are color projectors onto the color singlet and color octet states, and \mathcal{E}_α and $\mathcal{E}_{\alpha\beta}$ represent the polarization vector and tensor of the $c\bar{c}$ states, respectively.

Then the LO short distance cross section for the partonic process $i(p_1)j(p_2) \rightarrow c\bar{c}[n](p_3) + Z^0(p_4)$ is obtained by using the following formula:

$$\hat{\sigma}(ij \rightarrow c\bar{c}[n] + Z^0) = \frac{1}{16\pi\hat{s}^2} \int_{\hat{t}_{min}}^{\hat{t}_{max}} dt \overline{\sum} |\mathcal{A}_{LO}|^2, \quad (ij = u\bar{u}, d\bar{d}, s\bar{s}, gg). \quad (2.3)$$

The summation is taken over the spins and colors of initial and final states, and the bar over the summation denotes averaging over the spins and colors of initial partons. The Mandelstam variables are defined as: $\hat{s} = (p_1 + p_2)^2$, $\hat{t} = (p_1 - p_3)^2$, $\hat{u} = (p_1 - p_4)^2$.

The LO cross section for the $pp \rightarrow J/\psi + Z^0 + X$ process is expressed as

$$\begin{aligned} \sigma(pp \rightarrow J/\psi + Z^0 + X) &= \sum_{i,j,n} \frac{1}{1 + \delta_{ij}} \int dx_1 dx_2 \hat{\sigma}(ij \rightarrow c\bar{c}[n] + Z^0) \frac{\langle \mathcal{O}_n^{J/\psi} \rangle}{N_{col} N_{pol}} \\ &\times [G_{i/A}(x_1, \mu_f) G_{j/B}(x_2, \mu_f) + (A \leftrightarrow B)], \end{aligned} \quad (2.4)$$

where $G_{i,j/A,B}$ are the parton distribution functions (PDFs). A and B refer to protons at the LHC, N_{col} and N_{pol} refer to the numbers of colors and polarization states separately [48].

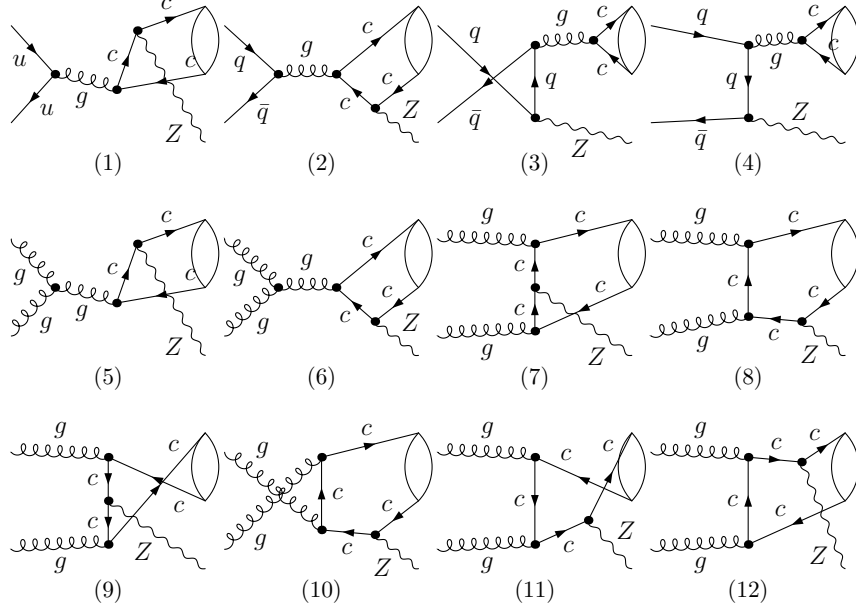


Figure 1: The tree-level Feynman diagrams for the partonic processes $q\bar{q} \rightarrow J/\psi + Z^0$ (1-4) and $gg \rightarrow J/\psi + Z^0$ (5-12).

The hadronic matrix elements $\langle \mathcal{O}_n^{J/\psi} \rangle$ are related to the hadronization from the states $c\bar{c}[n]$ into J/ψ which are fully governed by the nonperturbative QCD effects. The indices i, j run over all the partonic species and n denotes the specific color, spin and angular momentum $c\bar{c}$ -state.

Our numerical calculation shows that the main contributions come from the $gg \rightarrow c\bar{c}[^3S_1^{(1)}] + Z^0$ and $q\bar{q} \rightarrow c\bar{c}[^3S_1^{(8)}] + Z^0$ partonic processes. The contributions from other partonic processes are relative small. Therefore, we consider only the NLO QCD corrections to the $gg \rightarrow c\bar{c}[^3S_1^{(1)}] + Z^0$ and $q\bar{q} \rightarrow c\bar{c}[^3S_1^{(8)}] + Z^0$ partonic processes in the following NLO calculation.

3. NLO QCD corrections to the $pp \rightarrow J/\psi + Z^0 + X$ process

In our NLO QCD calculations we consider the following contribution components for the $pp \rightarrow J/\psi + Z^0 + X$ process:

- ▶ the virtual corrections to the partonic process $g(p_1)g(p_2) \rightarrow c\bar{c}[^3S_1^{(1)}](p_3) + Z^0(p_4)$ and $q(p_1)\bar{q}(p_2) \rightarrow c\bar{c}[^3S_1^{(8)}](p_3) + Z^0(p_4)$.
- ▶ the real gluon emission partonic processes $g(p_1)g(p_2) \rightarrow c\bar{c}[^3S_1^{(1)}](p_3) + Z^0(p_4) + g(p_5)$, $q(p_1)\bar{q}(p_2) \rightarrow c\bar{c}[^3S_1^{(1)}](p_3) + Z^0(p_4) + g(p_5)$ and $q(p_1)\bar{q}(p_2) \rightarrow c\bar{c}[^3S_1^{(8)}](p_3) + Z^0(p_4) + g(p_5)$.
- ▶ the real light-(anti)quark emission partonic processes $q(\bar{q})(p_1)g(p_2) \rightarrow c\bar{c}[^3S_1^{(1)}](p_3) + Z^0(p_4) + q(\bar{q})(p_5)$ and $q(\bar{q})(p_1)g(p_2) \rightarrow c\bar{c}[^3S_1^{(8)}](p_3) + Z^0(p_4) + q(\bar{q})(p_5)$.
- ▶ the collinear counterterms of the PDFs.

3.1 virtual corrections

The QCD $\mathcal{O}(\alpha_s)$ virtual corrections come from the one-loop diagrams including self-energy, vertex, box, pentagon and counterterm diagrams. Some representative one-loop Feynman

diagrams are displayed in Fig.2. We use FeynArts to generate the diagrams for all related subprocesses [49]. Then we use our in-house Mathematica program to simplify and square the amplitudes. The phase space integration is implemented by applying FormCalc programs [50]. There are UV, IR and Coulomb singularities in the the virtual corrections. We adopt the dimensional regularization (DR) scheme to regularize the UV and IR divergences, and the modified minimal subtraction $\overline{\text{MS}}$ and on-mass-shell schemes to renormalize the strong coupling constant and the quark wave functions, respectively. We adopt the definitions of one-loop integral functions in Ref [51,52], and use the Passarino-Veltman reduction formulas to reduce the tensor integrals to scalar integrals.

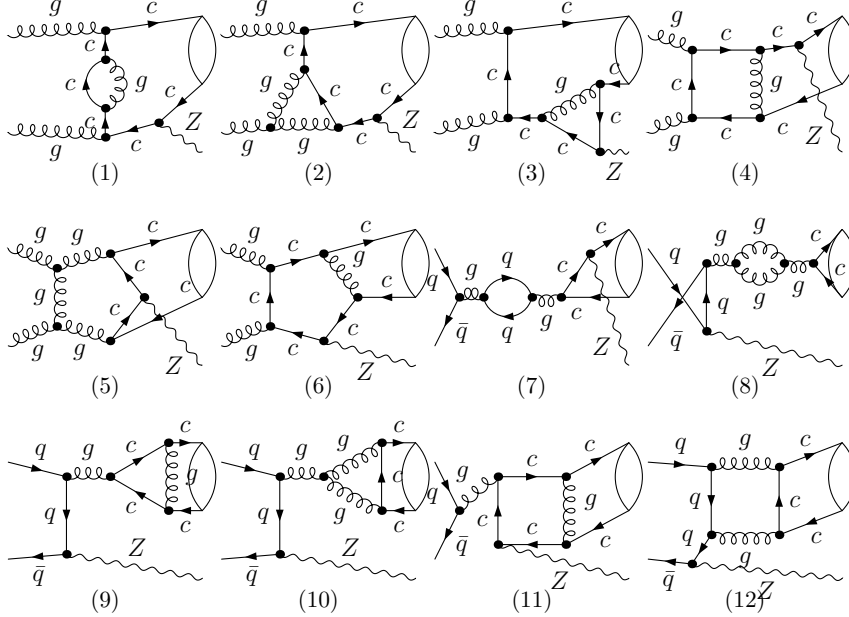


Figure 2: Some representative QCD one-loop Feynman diagrams for the partonic processes $gg \rightarrow c\bar{c}[{}^3S_1^{(1)}] + Z^0$ (1-6) and $q\bar{q} \rightarrow c\bar{c}[{}^3S_1^{(8)}] + Z^0$ (7-12).

We use the expressions in Ref. [53] to deal with the IR singularities in Feynman integrals, and apply the expressions in Refs. [54–56] to implement the numerical evaluations for the finite parts of N-point scale integrals. In the virtual correction calculations, we find that Fig.2(6,9,11) contain Coulomb singularities, which are regularized by a small relative velocity v between c and \bar{c} [57], and are canceled by those stemming from the NLO QCD correction to the operator $\langle \mathcal{O}_n^{J/\psi} \rangle$.

3.2 Real gluon/light-(anti)quark emission corrections

For the real emission partonic processes, there are IR singularities in the phase space integration. We use the two cutoff phase space slicing method (TCPSS) to perform the integration over the phase space of these real emission partonic processes [58]. In our calculations, the real gluon emission correction contains both soft and collinear IR singularities, which are isolated in soft gluon region ($E_5 \leq \delta_s \sqrt{\hat{s}}/2$) and hard gluon region ($E_5 > \delta_s \sqrt{\hat{s}}/2$) respectively. It is easy to find that soft singularities caused by the diagrams emitting soft gluon from the charm-quark and anti-charm-quark respectively in J/ψ are canceled

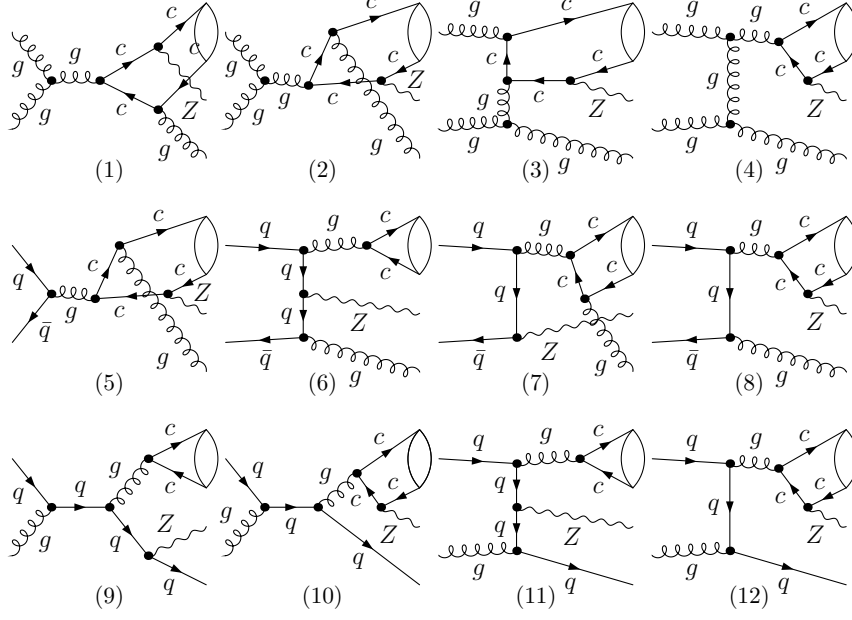


Figure 3: Some representative Feynman diagrams for real gluon/light-(anti)quark emission partonic processes.

with each other. The hard gluon region is divided into the hard collinear region (HC), i.e., $-\hat{t}_{15}$ (or $-\hat{t}_{25}$) $< \delta_c \hat{s}$, and the hard noncollinear region (\overline{HC}), i.e., $-\hat{t}_{15}$ (and $-\hat{t}_{25}$) $> \delta_c \hat{s}$ where $\hat{t}_{15} \equiv (p_1 - p_5)^2$ and $\hat{t}_{25} \equiv (p_2 - p_5)^2$. Each of the real light-(anti)quark emission processes contains only collinear IR singularity, and can be dealt with in the hard collinear region too. In the \overline{HC} region, the real emission corrections are finite and can be calculated numerically with general Monte Carlo method. After summing the virtual and real gluon/light-(anti)quark radiation corrections, the remained collinear divergence can be cancelled by the collinear counterterms of the PDFs. By adding all the contributions together, a finite total cross section is obtained.

The cross sections for the partonic processes $gg \rightarrow c\bar{c}[{}^3S_1^{(1)}] + Z^0 + g$ and $q\bar{q} \rightarrow c\bar{c}[{}^3S_1^{(8)}] + Z^0 + g$ in the soft region can be expressed as

$$\hat{\sigma}^S \left(gg \rightarrow c\bar{c}[{}^3S_1^{(1)}] + Z^0 + g \right) = -\frac{\alpha_s}{2\pi} \cdot (-3) \cdot g(p_1, p_2) \hat{\sigma}_{LO}[{}^3S_1^{(1)}], \quad (3.1)$$

$$\begin{aligned} \hat{\sigma}^S \left(q\bar{q} \rightarrow c\bar{c}[{}^3S_1^{(8)}] + Z^0 + g \right) &= -\frac{\alpha_s}{2\pi} \left[\frac{1}{6} g(p_1, p_2) - \frac{7}{6} (g(p_1, p_c) + g(p_2, p_{\bar{c}})) \right. \\ &\quad \left. - \frac{1}{3} (g(p_1, p_{\bar{c}}) + g(p_2, p_c)) \right] \hat{\sigma}_{LO}[{}^3S_1^{(8)}], \end{aligned} \quad (3.2)$$

where $g(p_i, p_j)$ is soft integral function defined as [59–62]

$$g(p_i, p_j) = \frac{(2\pi\mu)^{2\epsilon}}{2\pi} \int_{E_5 \leq \delta_s \sqrt{\hat{s}}/2} \frac{d^{D-1}p_5}{E_5} \left[\frac{2(p_i p_j)}{(p_i p_5)(p_j p_5)} - \frac{p_i^2}{(p_i p_5)^2} - \frac{p_j^2}{(p_j p_5)^2} \right], \quad (3.3)$$

while the cross section of partonic process $q\bar{q} \rightarrow c\bar{c}[{}^3S_1^{(1)}] + Z^0 + g$ is finite and can be evaluated directly in four-dimension using Monte Carlo method.

The collinear counterterms of the PDFs, $\delta G_{i/P}(x, \mu_f)$ ($P = p$; $i = g, u, \bar{u}, d, \bar{d}, s, \bar{s}$) contains two parts. One is the collinear gluon emission part $\delta G_{i/P}^{(gluon)}(x, \mu_f)$, another is the collinear light-(anti)quark emission part $\delta G_{i/P}^{(quark)}(x, \mu_f)$. Their analytical expressions are presented as follows.

$$\delta G_{q(g)/P}(x, \mu_f) = \delta G_{q(g)/P}^{(gluon)}(x, \mu_f) + \delta G_{q(g)/P}^{(quark)}(x, \mu_f), \quad (q = u, \bar{u}, d, \bar{d}, s, \bar{s}), \quad (3.4)$$

where

$$\begin{aligned} \delta G_{q(g)/P}^{(gluon)}(x, \mu_f) &= \frac{1}{\epsilon} \left[\frac{\alpha_s}{2\pi} \frac{\Gamma(1-\epsilon)}{\Gamma(1-2\epsilon)} \left(\frac{4\pi\mu_r^2}{\mu_f^2} \right)^\epsilon \right] \int_z^1 \frac{dz}{z} P_{qq(gg)}(z) G_{q(g)/P}(x/z, \mu_f), \\ \delta G_{q/P}^{(quark)}(x, \mu_f) &= \frac{1}{\epsilon} \left[\frac{\alpha_s}{2\pi} \frac{\Gamma(1-\epsilon)}{\Gamma(1-2\epsilon)} \left(\frac{4\pi\mu_r^2}{\mu_f^2} \right)^\epsilon \right] \int_z^1 \frac{dz}{z} P_{qg}(z) G_{g/P}(x/z, \mu_f), \\ \delta G_{g/P}^{(quark)}(x, \mu_f) &= \frac{1}{\epsilon} \left[\frac{\alpha_s}{2\pi} \frac{\Gamma(1-\epsilon)}{\Gamma(1-2\epsilon)} \left(\frac{4\pi\mu_r^2}{\mu_f^2} \right)^\epsilon \right] \sum_{q=u, \bar{u}}^{d, \bar{d}, s, \bar{s}} \int_z^1 \frac{dz}{z} P_{gq}(z) G_{q/P}(x/z, \mu_f). \end{aligned} \quad (3.5)$$

The soft and collinear IR singularities from virtual corrections can be canceled partially by adding with the contributions of the real gluon/light-(anti)quark emission processes and the gluon emission part of the PDF counterterms $\delta G_{q(g)/P}^{(gluon)}$. And the remaining collinear IR singularity can be canceled by the contributions of the collinear light-(anti)quark emission part of the PDF counterterms $\delta G_{q(g)/P}^{(quark)}$ exactly. All these cancelations are verified numerically in our numerical calculations. The explicit expressions for the splitting functions $P_{ij}(z)$, ($ij = qq, qg, gq, gg$) can be found in Ref. [58].

3.3 NLO QCD corrected cross sections

The NLO QCD corrected hadronic cross section for $J/\psi + Z^0$ associated production at the LHC can be written as

$$\sigma^{QCD} = \sigma^0 + \Delta\sigma^{QCD} = \sigma^0 + \Delta\sigma_{3S_1^{(1)}}^{gg} + \Delta\sigma_{3S_1^{(1)}}^{q\bar{q}} + \Delta\sigma_{3S_1^{(8)}}^{q\bar{q}} \quad (3.6)$$

The NLO QCD correction $\Delta\sigma^{QCD}$ contains three components: (1) $\Delta\sigma_{3S_1^{(1)}}^{gg}$, the NLO QCD correction to the subprocess $gg \rightarrow c\bar{c}[^3S_1^{(1)}] + Z^0$, (2) $\Delta\sigma_{3S_1^{(1)}}^{q\bar{q}}$, the NLO QCD correction to the subprocess $q\bar{q} \rightarrow c\bar{c}[^3S_1^{(1)}] + Z^0$, (3) $\Delta\sigma_{3S_1^{(8)}}^{q\bar{q}}$, the NLO QCD correction to the subprocess $q\bar{q} \rightarrow c\bar{c}[^3S_1^{(8)}] + Z^0$. Due to the absence of the LO cross section for the $q\bar{q} \rightarrow c\bar{c}[^3S_1^{(1)}] + Z^0$, the $\Delta\sigma_{3S_1^{(8)}}^{q\bar{q}}$ contains only the contribution of subprocess $q\bar{q} \rightarrow c\bar{c}[^3S_1^{(1)}] + Z^0 + g$.

The $\Delta\sigma_{3S_1^{(1)}}^{gg}$ and $\Delta\sigma_{3S_1^{(8)}}^{q\bar{q}}$ can be expressed as:

$$\Delta\sigma_{3S_1^{(1)}}^{gg} = \sigma_V^{(gg)} + \sigma_R^{(gg)g} + \sigma_R^{(gg)q} + \sigma_R^{(gg)\bar{q}}, \quad (3.7)$$

$$\Delta\sigma_{3S_1^{(8)}}^{q\bar{q}} = \sigma_V^{(q\bar{q})} + \sigma_R^{(q\bar{q})g} + \sigma_R^{(q\bar{q})q} + \sigma_R^{(q\bar{q})\bar{q}}, \quad (3.8)$$

where $\sigma_V^{(ij)}$, $\sigma_R^{(ij)g}$, $\sigma_R^{(ij)q}$ and $\sigma_R^{(ij)\bar{q}}$ ($ij = gg, q\bar{q}$) represent the virtual, the real gluon emission, the real light-quark and light-antiquark emission corrections to the cross section, respectively.

4. Numerical results and discussion

As a check of the correctness of our calculations, we compare our LO numerical results with the previous work in Ref. [45]. We adopt the same input parameters as in Ref. [45], and reproduce the LO distribution of $p_T^{J/\psi}$ which is in good agreement with that shown in Fig.5(a) of Ref. [45].

In the following numerical calculations for the $pp \rightarrow J/\psi + Z^0 + X$ process at the LHC, we take CTEQ6L1 PDFs with the one-loop running α_s in the LO calculations and CTEQ6M PDFs with the two-loop α_s in the NLO calculations [63]. For the QCD parameters we take the number of active flavor as $n_f = 3$, and input $\Lambda_{\text{QCD}}^{(3)} = 249$ MeV for the LO and $\Lambda_{\text{QCD}}^{(3)} = 389$ MeV for the NLO calculations [23], respectively. The renormalization, factorization, and NRQCD scales are taken as $\mu_r = \mu_f = m_T$ and $\mu_\Lambda = m_c$, respectively, where $m_T = \sqrt{\left(p_T^{J/\psi}\right)^2 + m_{J/\psi}^2}$ is the J/ψ transverse mass. The masses of the external particles and the fine structure constant are taken as $m_Z = 91.1876$ GeV, $m_c = m_{J/\psi}/2 = 1.5$ GeV and $\alpha = 1/137.036$. The $\langle \mathcal{O}^{J/\psi}[{}^3P_J^{(8)}] \rangle$ ($J = 0, 1, 2$) LDMEs satisfy the multiplicity relations

$$\langle \mathcal{O}^{J/\psi}[{}^3P_J^{(8)}] \rangle = (2J + 1) \langle \mathcal{O}^{J/\psi}[{}^3P_0^{(8)}] \rangle,$$

and the linear combination exists as

$$M_r^{J/\psi} = \langle \mathcal{O}^{J/\psi}[{}^1S_0^{(8)}] \rangle + \frac{r}{m_c^2} \langle \mathcal{O}^{J/\psi}[{}^3P_0^{(8)}] \rangle.$$

We take the LDMEs $\langle \mathcal{O}^{J/\psi}[{}^3S_1^{(1)}] \rangle = 1.3$ GeV³, $\langle \mathcal{O}^{J/\psi}[{}^3S_1^{(8)}] \rangle = 2.73 \times 10^{-3}$ GeV³, $M_r^{J/\psi} = 5.72 \times 10^{-3}$ GeV³ and $r = 3.54$ as the input parameters, which were fitted to the Tevatron RUN-I data by using the CTEQ4 PDFs and taking into account the dominant higher-order effects due to the multiple-gluon radiation in the inclusive J/ψ hadroproduction [64]. Then we fix the $\langle \mathcal{O}^{J/\psi}[{}^1S_0^{(8)}] \rangle$ and $\langle \mathcal{O}^{J/\psi}[{}^3P_0^{(8)}] \rangle$ LDMEs by the democratic choice [65, 66]

$$\langle \mathcal{O}^{J/\psi}[{}^1S_0^{(8)}] \rangle = \frac{r}{m_c^2} \langle \mathcal{O}^{J/\psi}[{}^3P_0^{(8)}] \rangle = \frac{1}{2} M_r^{J/\psi}.$$

We have checked numerically the independence of the total NLO QCD correction on the cutoffs δ_s and δ_c in the range $1 \times 10^{-4} \leq \delta_s \leq 1 \times 10^{-2}$ and $\delta_c = \delta_s/50$. The independence exists in our numerical results within the error tolerance. In further calculations, the two phase space cutoffs are fixed as $\delta_s = 1 \times 10^{-3}$ and $\delta_c = \delta_s/50$. Considering the validity of the NRQCD and perturbation method, we restrict our results to the domain $p_T^{J/\psi} > 3$ GeV and $|y_{J/\psi}| < 3$.

The dependence of the cross section on the renormalization scale μ_r and factorization scale μ_f induces uncertainty for theoretical prediction. In Fig.4, the μ dependence of the

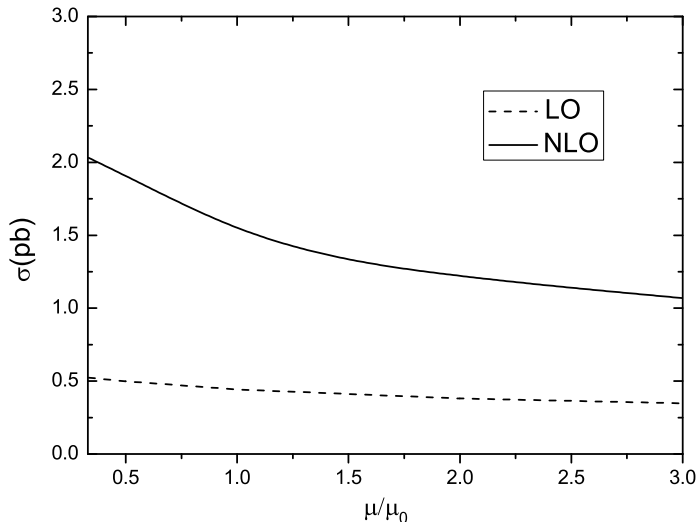


Figure 4: The dependence of the LO and the NLO QCD corrected cross sections for the process $pp \rightarrow J/\psi + Z^0 + X$ on the factorization scale and renormalization scale (μ/μ_0) at the LHC where we define $\mu = \mu_f = \mu_r$ and $\mu_0 = m_T$.

LO and the NLO QCD corrected cross sections with the constraints of $p_t^{J/\psi} > 3\text{GeV}$ and $|y_{J/\psi}| < 3$ for $pp \rightarrow J/\psi + Z^0 + X$ process, is shown with our default choice $\mu = \mu_r = \mu_f$ and the definition of $\mu_0 = m_T$. There μ varies from $\mu_0/3$ to $3\mu_0$. Not like the usual expectation, Fig.4 shows that the NLO QCD correction can not improve the LO scale independence for the $pp \rightarrow J/\psi + Z^0 + X$ process at the LHC. Actually, the similar behavior appears also in the results at the NLO in NRQCD (see Ref. [19]). The related theoretical uncertainty amounts to ${}_{-14}^{+13}\%$ at the LO and to ${}_{-21}^{+23}\%$ at the NLO when μ goes from $\mu_0/2$ to $2\mu_0$.

In Fig.5, we present the LO and NLO QCD corrected distributions of $p_T^{J/\psi}$ and the corresponding K-factors for the $pp \rightarrow J/\psi + Z^0 + X$ process at the LHC. For comparison, we also depict the LO and NLO QCD contributions from the $c\bar{c}[{}^3S_1^{(1)}]$ and $c\bar{c}[{}^3S_1^{(8)}]$ Fock states and their corresponding K-factors in these figures separately. The upper figure shows that the differential cross sections at the LO are significantly enhanced by the NLO QCD corrections and both the LO and NLO QCD corrected differential cross section curves drop rapidly with the increment of $p_T^{J/\psi}$. We can read out from the figure that the LO differential cross section of $p_T^{J/\psi}$ decreases from 79.2 fb/GeV to 0.3 fb/GeV and the NLO QCD corrected differential cross section of $p_T^{J/\psi}$ decreases from 221.1 fb/GeV to 1 fb/GeV as $p_T^{J/\psi}$ goes up from 3 to 50 GeV. The corresponding K-factor, defined as $K = \frac{d\sigma^{NLO}}{dp_T^{J/\psi}} / \frac{d\sigma^{LO}}{dp_T^{J/\psi}}$, varies in the range of [2.79, 3.42], and reach its maximum when $p_T^{J/\psi} = 50 \text{ GeV}$.

From Fig.5, we find that the contributions to the differential cross section from the $c\bar{c}[{}^3S_1^{(1)}]$ and $c\bar{c}[{}^3S_1^{(8)}]$ Fock states are comparable at lower $p_T^{J/\psi}$. As the $p_T^{J/\psi}$ increases, the contribution of $c\bar{c}[{}^3S_1^{(1)}]$ decreases much faster than $c\bar{c}[{}^3S_1^{(8)}]$. In all the plotted $p_T^{J/\psi}$ range, the CO contributions to the differential cross section of the process of $pp \rightarrow J/\psi + Z^0 + X$ are

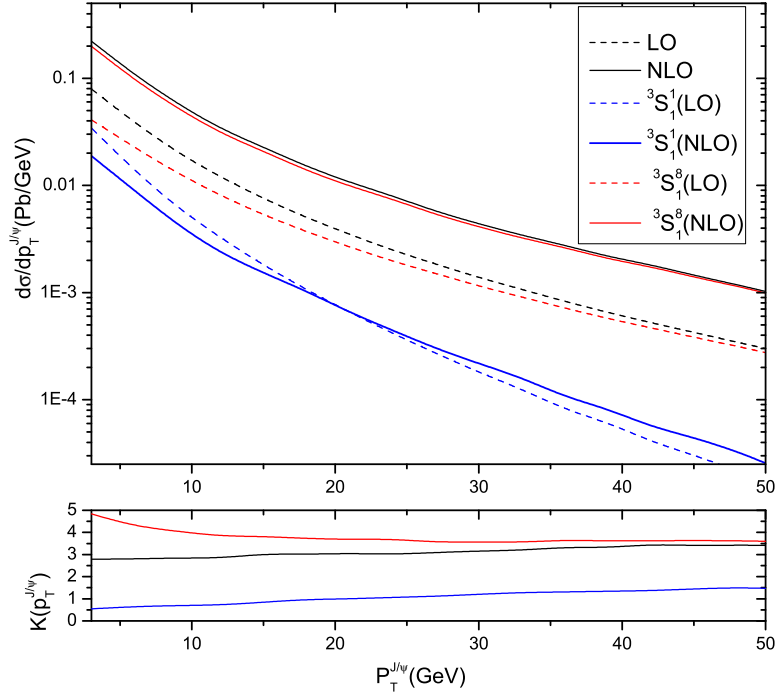


Figure 5: The LO and NLO QCD corrected distributions of $p_T^{J/\psi}$ and the corresponding K-factor for the $pp \rightarrow J/\psi + Z^0 + X$ process at the LHC.

dominant, and that will be beneficial to our study of CO mechanism. For the contribution from the $pp \rightarrow c\bar{c}[^3S_1^{(1)}] + Z^0 + X$ process, the K -factor of differential cross section increases from 0.55 to 1.50 as $p_T^{J/\psi}$ increases from 3 GeV to 50 GeV. As for the $pp \rightarrow c\bar{c}[^3S_1^{(8)}] + Z^0 + X$ process, the K -factor is larger than that for the $pp \rightarrow c\bar{c}[^3S_1^{(1)}] + Z^0 + X$ process, which decreases from 4.9 to 3.6 as $p_T^{J/\psi}$ increases from 3 GeV to 50 GeV.

5. Summary

The $J/\psi + Z^0$ associated production is an important process in investigating the production mechanism of J/ψ . In this paper we investigate the NLO QCD corrections to the $J/\psi + Z^0$ production at the LHC, and present the numerical predictions of the $p_T^{J/\psi}$ distribution of the $p_T^{J/\psi}$ up to the QCD NLO. We find that the LO differential cross section for the process $pp \rightarrow J/\psi + Z^0 + X$ is heavily enhanced by the NLO QCD corrections, and the K-factor can reach the value of 3.42 in the large $p_T^{J/\psi}$ region. The NLO QCD corrected differential cross section can reach 221.1 fb/GeV in the vicinity of $p_T^{J/\psi} \sim 3$ GeV. The process of $J/\psi + Z$ associated production is dominantly contributed by the CO mechanism in the large $p_T^{J/\psi}$ range. We conclude that the LHC has the potential to study the $J/\psi + Z^0$ production process, by which we can investigate the production mechanism of heavy quarkonium and extract the universal NRQCD matrix elements.

Acknowledgments: This work was supported in part by the National Natural Science Foundation of China(No.10875112, No.11075150, No.11005101), the Specialized Research Fund for the Doctoral Program of Higher Education(No.20093402110030), and the 211 Project of Anhui University.

References

- [1] M. B. Einhorn and S. D. Ellis, “Hadronic production of the new resonances: Probing gluon distributions,” *Phys. Rev. D* **12**, 2007 (1975).
- [2] S. D. Ellis, M. B. Einhorn, and C. Quigg, “Comment on Hadronic Production of Psions,” *Phys. Rev. Lett.* **36**, 1263 (1976).
- [3] C.-H. Chang, “Hadronic production of J/ψ associated with a gluon,” *Nucl. Phys. B* **172**, 425 (1980).
- [4] E. L. Berger and D. L. Jones, “Inelastic photoproduction of J/ψ and Υ by gluons ,” *Phys. Rev. D* **23**, 1521 (1981).
- [5] R. Baier and R. Ruckl, “On inelastic leptoproduction of heavy quarkonium states,” *Nucl. Phys. B* **201**, 1 (1982).
- [6] R. Barbieri, R. Gatto, and E. Remiddi, “Singular binding dependence in the hadronic widths of 1^{++} and 1^{+-} heavy quark antiquark bound,” *Phys. Lett. B* **61**, 465 (1976).
- [7] R. Barbieri, M. Caffo, R. Gatto, and E. Remiddi, “Strong QCD corrections to p-wave quarkonium decays,” *Phys. Lett. B* **95**, 93 (1980).
- [8] R. Barbieri, M. Caffo, R. Gatto, and E. Remiddi, “QCD corrections to P wave quarkonium decays,” *Nucl. Phys. B* **192**, 61 (1981).
- [9] R. Barbieri, E. d’Emilio, G. Curci, and E. Remiddi, “Strong radiative corrections to annihilations of quarkonia in QCD,” *Nucl. Phys. B* **154**, 535 (1979).
- [10] K. Hagiwara, C. B. Kim, and T. Yoshino, “Hadronic decay rate of ground-state para-quarkonia in quantum chromodynamics,” *Nucl. Phys. B* **177**, 461 (1981).
- [11] P. B. Mackenzie and G. P. Lepage, “Quantum Chromodynamic Corrections to the Gluonic Width of the Υ Meson,” *Phys. Rev. Lett.* **47**, 1244 (1981).
- [12] F. Abe et al. (CDF), “Inclusive J/ψ , $\psi(2S)$, and b-quark production in $p\bar{p}$ collisions at $\sqrt{s} = 1.8$ TeV,” *Phys. Rev. Lett.* **69**, 3704 (1992).
- [13] F. Abe et al. (CDF), “Inclusive χ_c and b-quark production in $p\bar{p}$ collisions at $\sqrt{s} = 1.8$ TeV ,” *Phys. Rev. Lett.* **71**, 2537 (1993).
- [14] G.T. Bodwin, E. Braaten, and G.P. Lepage, “Rigorous QCD analysis of inclusive annihilation and production of heavy quarkonium,” *Phys. Rev. D* **51**, 1125 (1995); **55**, 5853(E) (1997).
- [15] G.P. Lepage, L. Magnea, C. Nakhleh, U. Magnea, and K. Hornbostel, “Improved nonrelativistic QCD for heavy-quark physics,” *Phys. Rev. D* **46**, 4052 (1992).
- [16] E. Braaten and S. Fleming, “Color-Octet Fragmentation and the ψ' Surplus at the Fermilab Tevatron,” *Phys. Rev. Lett.* **74**, 3327 (1995).
- [17] B. Gong, X.Q. Li, J.X. Wang, “QCD corrections to J/ψ production via color-octet states at the Tevatron and LHC,” *Phys. Lett. B* **673**, (2009), 197.

- [18] Y.Q. Ma, K. Wang, K.T. Chao, “ $J/\psi(\psi')$ production at Tevatron and LHC at $O(\alpha_s^4 v^4)$ in nonrelativistic QCD,” hep-ph/1009.3655.
- [19] M. Butenschoen, B.A. Kniehl, “Reconciling J/ψ production at HERA, RHIC, Tevatron, and LHC with NRQCD factorization at next-to-leading order,” hep-ph/1009.5662.
- [20] J. Abdallah *et al.* (DELPHI Collaboration), “Study of inclusive J/ψ production in two-photon collisions at LEP II with the DELPHI detector ,” Phys. Lett. **B 565**, 76 (2003).
- [21] M. Klasen, B.A. Kniehl, L.N. Mihaila, and M. Steinhauser, “ Evidence for the Color-Octet Mechanism from CERN LEP2 $\gamma\gamma \rightarrow J/\psi + X$ Data,” Phys. Rev. Lett. **89**, 032001 (2002).
- [22] C. Adloff *et al.* (H1 Collaboration), “Inelastic Photoproduction of J/Psi Mesons at HERA ,” Eur. Phys. J. **C 25**, 25 (2002); M. Steder, on behalf of the H1 Collaboration, Report No. H1prelim-07-172.
- [23] M. Butenschon and B.A. Kniehl, “Complete Next-to-Leading-Order Corrections to J/ψ Photoproduction in Nonrelativistic Quantum Chromodynamics,” Phys. Rev. Lett. **104**, 072001 (2010).
- [24] Y. J. Zhang, Y. j. Gao and K. T. Chao, “Next-to-Leading-Order QCD Correction to $e^+e^- \rightarrow J/\psi + \eta_c$ at $\sqrt{s} = 10.6$ GeV,” Phys. Rev. Lett. **96**, 092001 (2006).
- [25] Y. J. Zhang and K. T. Chao, “Double-Charm Production $e^+e^- \rightarrow J/\psi + c\bar{c}$ at B Factories with Next-to-Leading-Order QCD Corrections,” Phys. Rev. Lett. **98**, 092003 (2007).
- [26] Y. J. Zhang, Y. Q. Ma and K. T. Chao, “Factorization and next-to-leading-order QCD correction in $e^+e^- \rightarrow J/\psi(\psi(2S)) + \chi_{c0}$,” Phys. Rev. **D 78**, 054006 (2008).
- [27] Y. Q. Ma, Y. J. Zhang and K. T. Chao, “QCD Corrections to $e^+e^- \rightarrow J/\psi + gg$ at B Factories,” Phys. Rev. Lett. **102**, 162002 (2009).
- [28] B. Gong and J. X. Wang, “QCD corrections to J/ψ plus η_c production in e^+e^- annihilation at $\sqrt{s} = 10.6$ GeV,” Phys. Rev. **D 77**, 054028 (2008).
- [29] B. Gong and J. X. Wang, “QCD Corrections to Double J/ψ Production in e^+e^- Annihilation at $\sqrt{s} = 10.6$ GeV,” Phys. Rev. Lett. **100**, 181803 (2008).
- [30] B. Gong and J. X. Wang, “Next-to-Leading-Order QCD Corrections to $e^+e^- \rightarrow J/\psi + gg$ at B Factories,” Phys. Rev. Lett. **102**, 162003 (2009).
- [31] W. L. Sang and Y. Q. Chen, “Higher order corrections to the cross section of $e^+e^- \rightarrow$ quarkonium + γ ,” Phys. Rev. **D 81**, 034028 (2010), hep-ph/0910.4071.
- [32] D. Li, Z. G. He and K. T. Chao, “Search for $C = +$ charmonium and bottomonium states in $e^+e^- \rightarrow \gamma + X$ at B factories,” Phys. Rev. **D 80**, 114014 (2009).
- [33] Y. J. Zhang, Y. Q. Ma, K. Wang and K. T. Chao, “QCD radiative correction to color-octet J/ψ inclusive production at B factories,” Phys. Rev. **D 81**, 034015 (2010).
- [34] B.Gong and J. X. Wang, “Next-to-leading-order QCD corrections to $e^+e^- \rightarrow J/\psi c\bar{c}$ at the B factories,” Phys. Rev. **D 80**, 054015 (2009).
- [35] G.T. Bodwin, D. Kang, T. Kim, J. Lee and C. Yu, “Relativistic Corrections to $e^+e^- \rightarrow J/\psi + \eta_c$ in a Potential Model,” AIP Conf. Proc. **892**, 315 (2007).
- [36] Z. G. He, Y. Fan and K. T. Chao, “Relativistic corrections to J/ψ exclusive and inclusive double charm production at B factories,” Phys. Rev. **D 75**, 074011 (2007).

- [37] G. T. Bodwin, J. Lee and C. Yu, “Resummation of relativistic corrections to $e^+e^- \rightarrow J/\psi + \eta_c$,” Phys. Rev. **D 77**, 094018 (2008).
- [38] Z. G. He, Y. Fan and K. T. Chao, “Relativistic correction to $e^+e^- \rightarrow J/\psi + gg$ at B factories and constraint on color-octet matrix elements,” Phys. Rev. **D 81**, 054036 (2010).
- [39] Y. Jia, “Color-singlet relativistic correction to inclusive J/ψ production associated with light hadrons at B factories,” Phys. Rev. **D 82**, 034017 (2010), hep-ph/0912.5498.
- [40] E. Braaten, B. A. Kniehl, and J. Lee, “Polarization of prompt J/ψ at the Fermilab Tevatron,” Phys. Rev. **D 62**, 094005 (2000).
- [41] B. A. Kniehl and J. Lee, “Polarized J/ψ from χ_{cJ} and ψ' decays at the Fermilab Tevatron,” Phys. Rev. **D 62**, 114027 (2000).
- [42] P. Artoisenet, J. Campbell, F. Maltoni, and F. Tramontano, “ J/ψ Production at HERA,” Phys. Rev. Lett. **102**, 142001 (2009).
- [43] V. Barger, S. Fleming, and R.J.N. Phillips, “Double gluon fragmentation to J/ψ pairs at the Tevatron,” Phys. Lett. **B 371**, 111 (1996).
- [44] E. Braaten, J. Lee, “Associated production of Υ and weak gauge bosons in hadron colliders,” Phys. Rev. **D 60**, 091501.
- [45] B.A. Kniehl, C.P. Palisoc, L. Zwirner, “Associated production of heavy quarkonia and electroweak bosons at present and future colliders,” Phys. Rev. **D 66** (2002) 114002, hep-ph/0208104.
- [46] R. Li, J.X. Wang, “Next-to-leading-order QCD corrections to $J/\psi(\Upsilon) + \gamma$ production at the LHC,” Phys. Lett. **B 672**, 51 (2009).
- [47] G. Li, M. Song, R.Y. Zhang, and W.G. Ma, “QCD corrections to J/ψ production in association with a W -boson at the LHC,” Phys. Rev. **D 83** (2011) 014001, arXiv:1012.3798.
- [48] A. Petrelli, M. Cacciari, M. Greco, F. Maltoni, and M.L. Mangano, “NLO production and decay of quarkonium,” Nucl. Phys. **B 514**, 245 (1998).
- [49] T. Hahn, “Generating Feynman diagrams and amplitudes with FeynArts,” Comput. Phys. Commun. **140** (2001) 418.
- [50] T. Hahn, M. Perez-Victoria, “Automated one-loop calculations in four and D dimensions,” Comput. Phys. Commun. **118** (1999) 153.
- [51] G. Passarino and M. Veltman, “One-loop corrections for e^+e^- annihilation into $\mu^+\mu^-$ in the Weinberg model,” Nucl. Phys. **B 160**, 151 (1979).
- [52] A. Denner and S. Dittmaier, “Reduction schemes for one-loop tensor integrals,” Nucl. Phys. **B 734** (2006) 62.
- [53] R.K. Ellis and G. Zanderighi, “Scalar one-loop integrals for QCD,” JHEP **0802**, 002 (2008).
- [54] G. 't Hooft and M. Veltman, “Scalar one-loop integrals,” Nucl. Phys. **B153**, 365 (1979).
- [55] A. Denner, U. Nierste, and R. Scharf, “A compact expression for the scalar one-loop four-point function,” Nucl. Phys. **B 367**, 637 (1991).
- [56] A. Denner and S. Dittmaier, “Reduction of one-loop tensor 5-point integrals,” Nucl. Phys. **B 658**, 175 (2003).

- [57] M. Kramer, “QCD corrections to inelastic J/ψ photoproduction,” Nucl. Phys. **B 459**, 3 (1996).
- [58] B.W. Harris and J.F. Owens, “Two cutoff phase space slicing method,” Phys. Rev. **D 65**, 094032 (2002).
- [59] W. Beenakker, H. Kuijf, W.L. van Neerven, and J. Smith, “QCD corrections to heavy-quark production in $p\bar{p}$ collisions,” Phys. Rev. **D 40**, 54 (1989).
- [60] J. Smith, D. Thomas, and W.L. van Neerven, “QCD corrections to the reaction $p + \bar{p} \rightarrow W + \gamma + X$,” Z. Phys. **C 44**, 267 (1989).
- [61] W.L. van Neerven, “Dimensional regularization of mass and infrared singularities in two-loop on-shell vertex functions,” Nucl. Phys. **B 268** (1986) 453.
- [62] B.W. Harris and J. Smith, “Heavy-quark correlations in deep-inelastic electroproduction,” Nucl. Phys. **B 452** (1995) 109.
- [63] J. Pumplin, D.R. Stump, J. Huston, H.L. Lai, P. Nadolsky, and W.K. Tung, “New Generation of Parton Distributions with Uncertainties from Global QCD Analysis,” JHEP **0207**, 012 (2002).
- [64] B.A. Kniehl and G. Kramer, “TEVATRON-HERA Color-Octet Charmonium Anomaly Versus Higher-Order QCD Effects,” Eur. Phys. J. **C 6**, 493 (1999).
- [65] M. Klasen, B.A. Kniehl, L.N. Mihaila, and M. Steinhauser, “ J/ψ plus jet associated production in two-photon collisions at next-to-leading order,” Nucl. Phys. **B 713**, 487 (2005).
- [66] M. Klasen, B.A. Kniehl, L.N. Mihaila, and M. Steinhauser, “ J/ψ plus prompt-photon associated production in two-photon collisions at next-to-leading order,” Phys. Rev. **D 71**, 014016 (2005).